

Laser-induced magnetization switching in synthetic-ferrimagnetic bilayer

V. N. Gridnev *

Ioffe Institute, 194021 St. Petersburg, Russia



(Received 29 August 2022; accepted 9 February 2023; published 21 February 2023)

We present a theoretical study of all-optical magnetization switching in rare-earth/transition-metal bilayer, RE_n/TM_m , consisting of n RE monolayers and m TM monolayers. Using the Landau-Lifshitz-Bloch equation, we numerically calculate the spin dynamics, including spin transport in the bilayer, upon incidence of a single laser pulse. It is shown that the spin transfer between the RE and TM layers with $n > 1$ or $m > 1$ is necessary for the switching. The calculation shows that the spin transfer makes conditions for the switching similar to those for the ferrimagnetic alloys. When the spin transfer between the monolayers is absent the intensity of the exchange scattering decreases and the switching is possible only in the RE_1/TM_1 bilayer. A relationship between the spin relaxation and temperature dependence of the switching is discussed.

DOI: [10.1103/PhysRevB.107.054428](https://doi.org/10.1103/PhysRevB.107.054428)

I. INTRODUCTION

Purely thermal single-pulse all-optical switching (AOS) of magnetization was first observed in ferrimagnetic metals, see Refs. [1–3] for a review. Later, AOS was also demonstrated in the synthetic-ferrimagnetic layered structures [4–6].

A distinctive feature of spin dynamics in magnetic heterostructures is the spin transport across the interfaces. It was shown experimentally that the spin transport significantly affects AOS in magnetic layered structures [7–10].

In this paper we will explore the possibility of thermally induced AOS in rare-earth/transition-metal (RE/TM) synthetic ferrimagnets composed of two ferromagnetic layers. We apply the s - d model to study the role of the spin transport in AOS in the synthetic-ferrimagnetic bilayer. The s - d model has already been used to investigate the interplay between the local magnetization dynamics and the spin transport in magnetic heterostructures [11]. However, the impact of spin transport on AOS has not been considered theoretically until now. This paper is aimed to fill this gap.

II. MODEL

We will model the synthetic ferrimagnetic bilayer composed of two RE and TM ferromagnetic layers with antiferromagnetic exchange coupling between them. In equilibrium, the spins in RE and TM layers are oriented antiparallel. The structure of the bilayer is labeled as RE_n/TM_m where the indices n and m correspond to the number of monolayers of each element. The RE and TM ions with spins (angular momenta) $S_{\text{RE}}=7/2$ and $S_{\text{TM}}=1$ (in units of \hbar) are embedded in the degenerate electron gas of density n_c forming a single band with energy E_{ks} , where k and s are the wave vector and spin, respectively.

We will consider the purely longitudinal spin dynamics and calculate the average spin polarization of localized spins S_i in monolayer i , $i = 1-N$, where $N \equiv n + m$. We neglect an external magnetic field and magnetocrystalline anisotropy, i.e., we take into account only the exchange interaction between spins. Thus, our problem possesses rotational symmetry. Therefore, we do not specify coordinate axes to simplify notations.

A localized spin S_i possesses $(2S_i + 1)$ discrete energy-levels E_m with the splitting δ_i which is determined by the exchange interaction with other spins by the relation [5],

$$\delta_i = \frac{J_{i,i-1}}{4} S_{i-1} + \frac{J_{i,i}}{2} S_i + \frac{J_{i,i+1}}{4} S_{i+1}, \quad (1)$$

where $J_{i,j}$ are the exchange coupling constants between the localized spins. For the first and last monolayers ($i = 1$ or N) the first or last term in Eq. (1) should be excluded. We set $J_{\text{TM-TM}} = 0.142$, $J_{\text{RE-RE}} = 0.05$, and $J_{\text{TM-RE}} = -0.05$ eV. Note that we include the numbers of nearest-neighbors $z_{i,j}$ in the definition of $J_{i,j}$. With these parameters the Curie temperatures of the bulk TM and RE ferromagnets are $T_{C,\text{TM}} = 1100$ and $T_{C,\text{RE}} = 300$ K. In equilibrium S_i satisfy the system of N equations,

$$S_i = S_\nu B_{S_\nu} \left(\frac{S_\nu \delta_i}{kT} \right), \quad (2)$$

where B_S is the Brillouin function and δ_i is given by Eq. (1). Here and in the following $\nu = \text{RE}$ (TM) when $i \in \text{RE}$ (TM) monolayer.

Parameters $J_{i,j}$ completely define an effective Heisenberg Hamiltonian and are sufficient for the calculation of the equilibrium spin polarizations of the localized spins. However, for the calculation of the spin polarization of itinerant spins as well as the longitudinal spin dynamics, we need parameters α_i of the exchange interaction between the localized and the itinerant spins.

*gridnev@mail.ioffe.ru

The s - d Hamiltonian is given by

$$\hat{H}_{sd} = \sum_{i,j} \alpha_i \delta(\mathbf{r}_j - \mathbf{R}_i) (\hat{\mathbf{S}}_i \cdot \hat{\mathbf{s}}_j), \quad (3)$$

where \mathbf{r}_j (\mathbf{R}_i) is the position of the carrier (localized spin) and α_i is the exchange coupling constant. In our calculation we set $n_c \alpha_{RE} = 0.01$ and $n_c \alpha_{TM} = 0.1$ eV.

Applying a mean-field approximation to the s - d Hamiltonian (3) one can obtain [12]

$$\delta_i = -n_c \alpha_i s_i, \quad (4)$$

where $s_i \equiv \langle \hat{s}(\mathbf{R}_i) \rangle$ is the spin density of the itinerant electrons in monolayer i . Comparing Eqs. (1) and (4) we obtain the equilibrium spin polarization of itinerant electrons,

$$s_i = \frac{\chi_{i,i-1}}{4} S_{i-1} + \frac{\chi_{i,i}}{2} S_i + \frac{\chi_{i,i+1}}{4} S_{i+1}, \quad (5)$$

where $\chi_{i,j} = J_{ij}/n_c \alpha_i$ is an electron spin susceptibility. Using Eqs. (2) and (5), we can calculate the reduced total spin polarization $P_{\text{tot}} = N^{-1} \sum_{i=1}^N (S_i + s_i)$. Obviously, P_{tot} consists of three parts: $P_{\text{tot}} = P_{\text{RE}} + P_{\text{TM}} + P_e$.

Dynamical equations

For the calculation of the longitudinal spin dynamics in the bilayer, we use the Landau-Lifshitz-Bloch (LLB) equation modified for magnetic metals [13],

$$\frac{dS_i}{dt} = C_i g_i S_i \left[\coth\left(\frac{y_i}{2}\right) - \coth\left(\frac{g_i}{2}\right) \right], \quad (6)$$

where $g_i = \beta_e [\delta_i(t) + \mu_{i\uparrow}(t) - \mu_{i\downarrow}(t)]$, $\beta_e = 1/k_B T_e(t)$,

$$C_i = \frac{2\pi}{\hbar} \alpha_i^2 k_B T_e D_{\uparrow}(E_F) D_{\downarrow}(E_F - \delta_i), \quad (7)$$

where E_F is the Fermi energy, T_e is the electron temperature, D_s and μ_{is} are the spin resolved density of states and electron's chemical potential, respectively. $y_i(t)$ is related to the average spin S_i by the relation,

$$S_i(t) = S_v B_{S_v} [S_v y_i(t)]. \quad (8)$$

In equilibrium $y_i = \delta_i/k_B T$.

Equation (6) has the same form as that derived for a ferromagnet in the previous works [14–16]. However, in contrast to those works the dynamics described by Eq. (6) is governed by the s - d interaction rather than the spin-lattice interaction. Due to the s - d interaction, this equation is coupled to the nonequilibrium spin polarization of the itinerant electrons.

In order to solve Eq. (6) for $S_i(t)$ one needs to know the functions $g_i(t)$. These functions depend on the electron temperature $T_e(t)$, average spins $S_i(t)$ (through δ_i), and the spin splitting of chemical potential,

$$\Delta\mu_i(t) = \mu_{i\uparrow} - \mu_{i\downarrow}.$$

In equilibrium $\Delta\mu_i = 0$, but after a photoexcitation $\Delta\mu_i \neq 0$, and becomes dependent on the monolayer position i in the bilayer.

We choose a simplified approach to the calculation of $\Delta\mu_i(t)$ and consider two limiting cases. First, we assume that there is no spin transfer between the two layers, i.e., the interface is nontransparent for the itinerant spins. The second

limiting case is that the interface is completely transparent for the spins. In both cases, we assume that the electron transport is ballistic.

In the ballistic regime $\Delta\mu_i(t)$ becomes spatially homogeneous within each layer on a timescale ~ 1 fs (if $N \lesssim 10$). Then $\Delta\mu_i(t)$ is completely determined by nonequilibrium values of spins $s_i(t)$ and $S_i(t)$. In the first case (the nontransparent interface), we set

$$\Delta\mu_i = n_c (s_i - s_i^e) \frac{D_{\uparrow}(E_F) + D_{\downarrow}(E_F)}{D_{\uparrow}(E_F) D_{\downarrow}(E_F)}, \quad (9)$$

where $s_i^e(t)$ is an instantaneous equilibrium value of the average electron spin s_z , determined by the electron temperature T_e and by the condition $\mu_{\uparrow} = \mu_{\downarrow}$ [12]. We define s_i^e as

$$s_i^e(t) = s_i[\{S_i(t)\}], \quad (10)$$

where $s_i[\{S_i(t)\}]$ are given by Eq. (5) with time-dependent $S_i(t)$. $\Delta\mu_i$, determined by Eq. (9), behaves as function of i , such as a step function, i.e., it possesses a discontinuity at the interface.

For the completely transparent interface and the ballistic transport, $\Delta\mu_i$ is independent of i . Therefore, we determine $\Delta\mu$ by averaging of Eq. (9) over all monolayers,

$$\Delta\mu = \frac{1}{N} \sum_i \Delta\mu_i, \quad (11)$$

where $\Delta\mu_i$ is given by Eq. (9). Although Eqs. (9) and (11) are obtained using the rough approximations, we believe that they allow us to understand the role of spin transport in the switching on a qualitative level.

The dynamics of the average itinerant spin, entering Eq. (9), is determined by the exchange scattering and spin-lattice relaxation,

$$\frac{ds_i}{dt} = -\frac{n_v}{n_c} \frac{dS_i}{dt} - \frac{[s_i - s_i^e(t)]}{\tau_{sl}}. \quad (12)$$

The first term on the right-hand side describes the exchange scattering, and the last term describes the spin-lattice relaxation of the electron spin with a relaxation time τ_{sl} . We set $n_c = 10^{23}$ cm $^{-3}$, $n_{\text{RE}}/n_c = n_{\text{RE}}/n_c = 1$, and $\tau_{sl} = 0.01$ ps. We choose the unrealistically short spin-lattice relaxation time to reveal better the role of fast spin-lattice relaxation in the switching, see below. The case of slow spin-lattice relaxation is simpler and was considered earlier [17,18].

The electron and phonon temperatures T_e and T_p , respectively, are governed by the equations,

$$C_e(T_e) \frac{dT_e}{dt} = -G_{ep}(T_e - T_p) + P(t), \quad (13)$$

$$C_p \frac{dT_p}{dt} = G_{ep}(T_e - T_p) - \frac{T_p - T}{\tau_p}, \quad (14)$$

where T is an initial temperature of the bilayer, G_{ep} is the electron-phonon coupling, and

$$P(t) = P_0 \exp[-(t/t_0)^2]$$

describes the time evolution of the laser energy transfer to the electrons. We assume that the laser pulse heats up the bilayer homogeneously. The last term in Eq. (14) describes

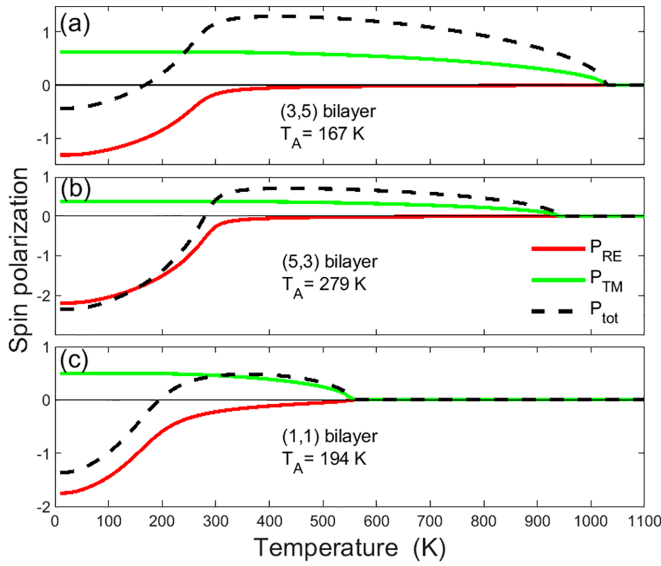


FIG. 1. Calculated temperature dependence of the equilibrium spin polarizations for different bilayers. Here and in the following the structure of the rare-earth/transition-metal bilayer is labeled as (n, m) or RE_n/TM_m , where n and m are the numbers of RE and TM monolayers, respectively.

heat diffusion to an environment. We take the laser pulse fluence $F_0 = P_0 t_0 \sqrt{\pi}$ as an input parameter.

Thus, Eqs. (6), (9), (11)–(14) describe the laser-induced spin dynamics in the bilayer.

To solve the LLB equation numerically, we set the specific heat of the phonons $C_p = 3 \times 10^6 \text{ J m}^{-3} \text{ K}^{-1}$ and the electrons $C_e = \gamma T_e$, where $\gamma = 700 \text{ J m}^{-3} \text{ K}^{-2}$. The densities of states for both spins are $D_\uparrow(E_F) = 2.5 \times 10^{23}$ and $D_\downarrow(E_F) = 2.5 \times 10^{23} \text{ cm}^{-3} \text{ eV}^{-1}$. We set the pulse duration $t_0 = 100 \text{ fs}$, the heat diffusion time $\tau_p = 20 \text{ ps}$, and the laser pulse fluence $F_0 = 0.4 \text{ GJ m}^{-3}$. With these parameters the maximum electron temperature $T_e^{\text{max}} \approx T_{C, \text{TM}} = 1100 \text{ K}$.

III. RESULTS

Figure 1 shows the equilibrium spin polarizations of RE and TM sublattices as well as the total spin polarization for different thicknesses of the RE and TM layers. All polarizations were calculated as the spatial average of the spins (angular momenta) over the volume of the sample. Recall, that $P_{\text{tot}} = P_{\text{RE}} + P_{\text{TM}} + P_e$. Note, that the RE layer exhibits magnetic ordering above its own bulk Curie temperature $T_{C, \text{RE}}$ due to the interaction with the TM layer.

If the number of TM monolayers m is not too large compared the number of RE monolayers n , then there is a compensation temperature T_A at which $P_{\text{tot}}(T_A) = 0$ [19]. This temperature is close to the angular momentum compensation temperature [18].

A. Transparent interface

The temperature T_A plays an important role in the switching in the bulk ferrimagnets [18]. In this section, we show that the same is true for the bilayer if the spin transport is ballistic, and the interface between the layers is transparent for

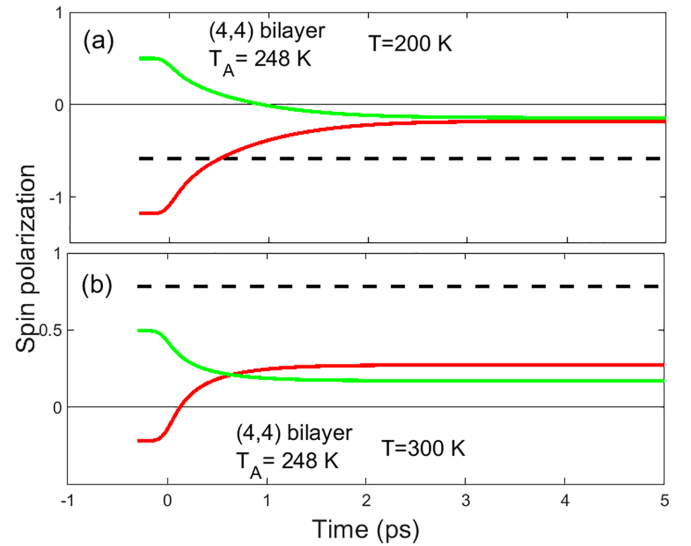


FIG. 2. Spin dynamics in the (4,4) bilayer with transparent interface without electron cooling and spin relaxation. (a) below and (b) above T_A . Red, green, and dashed curves represent P_{RE} , P_{TM} , and P_{tot} , respectively.

the itinerant spins. In this case, $\Delta\mu$ is given by Eq. (11). The simplest way to establish the possibility of switching is to investigate the occurrence of ferromagneticlike states [17]. To this end we eliminate the electron cooling and spin relaxation from the dynamical equations ($G_{ep} = 0$ and $\tau_s^{-1} = 0$) and retain only the s - d interaction. Figures 2(a) and 2(b) shows the calculated spin dynamics below and above the compensation temperature T_A , respectively. In both cases we see the appearance of ferromagneticlike states with different polarities. Now we take into account the electron cooling ($G_{ep} = 6 \times 10^{16} \text{ W m}^{-3} \text{ K}^{-1}$). Then, the ferromagneticlike states with the opposite polarities behave quite differently. The spin dynamics shown in Figs. 2(a) and 2(b) transforms into the spin dynamics shown in Figs. 3(a) and 3(b), respectively.

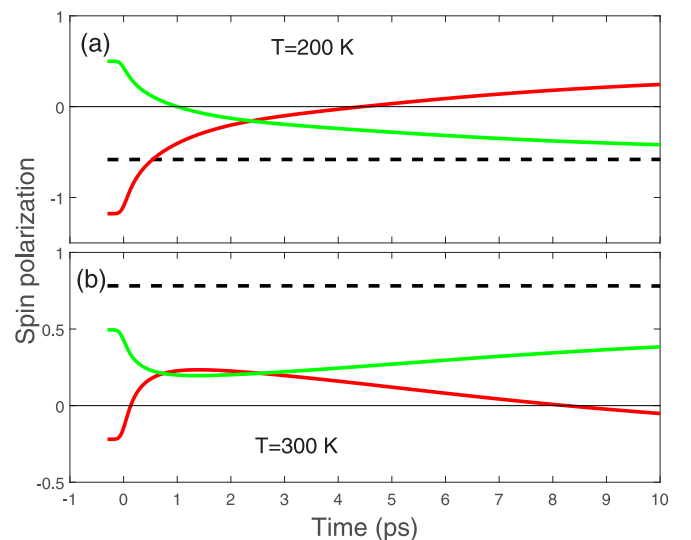


FIG. 3. The same as in Fig. 2 but with the electron cooling. The electron-phonon coupling $G_{ep} = 6 \times 10^{16} \text{ W m}^{-3} \text{ K}^{-1}$.

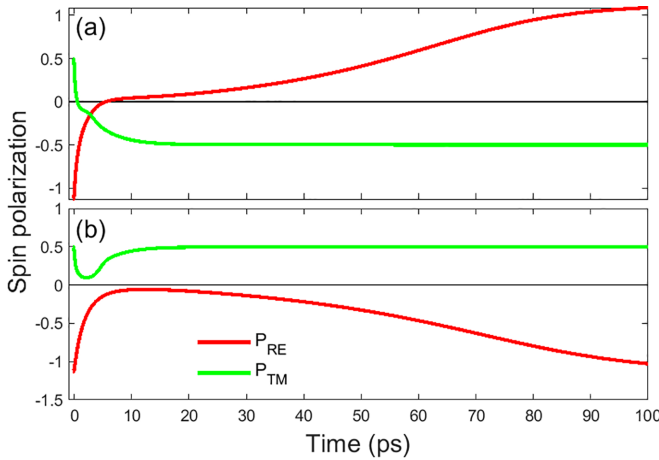


FIG. 4. Ultrafast switching and demagnetization of sublattice spin polarizations in the (3,3) bilayer. (a) Transparent interface and (b) nontransparent interface. The electron-phonon coupling $G_{ep} = 6 \times 10^{16} \text{ W m}^{-3} \text{ K}^{-1}$ and spin-lattice relaxation time $\tau_{sl} = 0.01 \text{ ps}$.

When P_{TM} changes sign [Fig. 2(a)] the electron cooling leads to the switching [Fig. 3(a)]. But the ferromagneticlike state with the opposite polarity [Fig. 2(b)] recovers to the initial state [Fig. 3(b)]. Thus, the switching occurs only below the compensation temperature T_A . Such temperature dependence of the switching is qualitatively similar to that in the bulk ferrimagnets [17]. This provides other evidence of the essential role of the exchange scattering in the switching. A more complicated situation occurs in the case when the interface is fully nontransparent for the itinerant spins.

B. Nontransparent interface

When the interface between the layers is fully nontransparent for the electron spins the spin splitting of the electron chemical potential is given by Eq. (9). Figures 4(a) and 4(b) shows the calculated spin dynamics for the transparent and nontransparent interface, respectively. It is seen that the switching occurs only if the interface is transparent for the electron spins. In the case of nontransparent interface the sublattice spin polarizations recover to the initial state after a partial demagnetization.

We performed the calculations for different numbers of monolayers n and m varying the initial temperature and other parameters of the system. Here we present only the results that illustrate the main trends. We found that in all bilayers, with the exception of the (1,1) bilayer, the switching does not occur if the interface is nontransparent.

Now we will consider a special case of the (1,1) bilayer when the interface is nontransparent, but the switching nevertheless occurs. In the case of nontransparent interface the exchange scattering is effective only near the interface and typically does not affect the spin transfer between the RE and the TM sublattices significantly. In the (1,1) bilayer the both layers are adjacent to the interface, and under certain conditions can undergo the switching. Note that in our model, we use the extremely short-range exchange interaction between the films, Eqs. (1) and (5). This is the reason why we observe the switching only of the (1,1) bilayer.

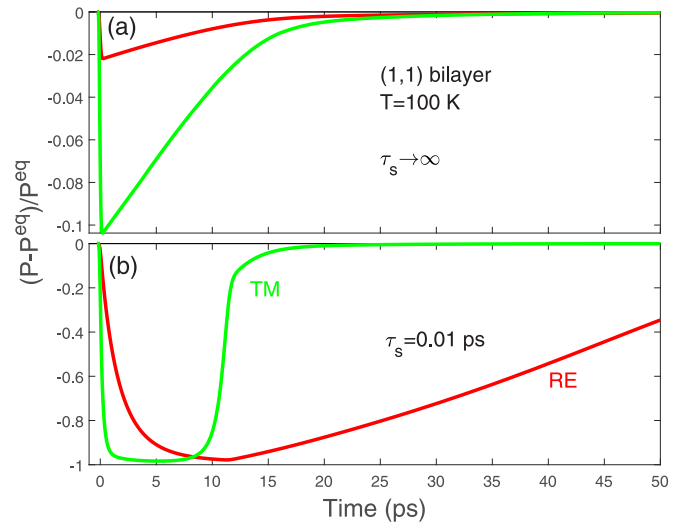


FIG. 5. Demagnetization of RE (red) and TM (green) spin polarizations in (1,1) bilayer ($T_A = 194 \text{ K}$) with nontransparent interface at $T = 100 \text{ K}$. (a) Without spin relaxation and (b) with spin relaxation.

Figure 5 shows the normalized deviation of RE and TM spin polarizations from equilibrium $D = (P - P^{eq})/P^{eq}$, without (a) and with (b) spin relaxation at $T = 100 \text{ K}$ [20]. It is seen that only demagnetization occurs. Comparing Figs. 5(a) and 5(b), one can see that the spin relaxation significantly affects demagnetization. When the spin relaxation slows down ($\tau_s \rightarrow \infty$), the degree of demagnetization decreases. When the spin transfer between the layers is slow the spin-lattice relaxation becomes the main mechanism of demagnetization.

When the initial temperature increases and becomes significantly higher than $T_A = 194 \text{ K}$ we unexpectedly observe the switching [Fig. 6(b)]. Again, comparing Figs. 6(a) and 6(b) one can see that the spin relaxation significantly affects

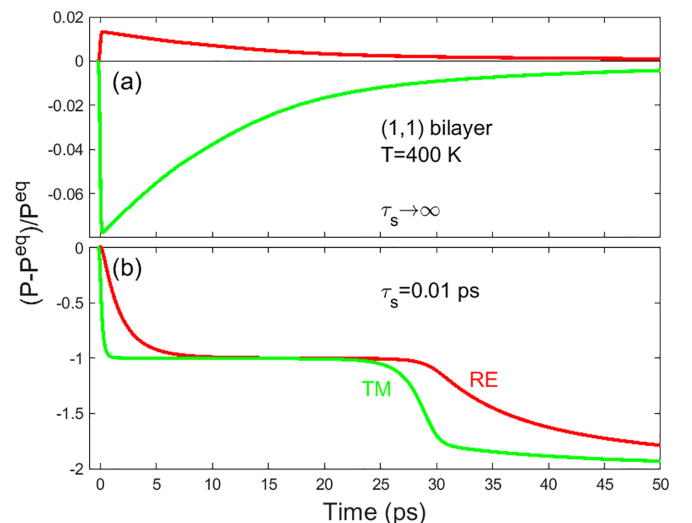


FIG. 6. The same as in Fig. 5 but at the initial temperature $T = 400 \text{ K}$.

the dynamics: with an increase in the spin-relaxation rate, demagnetization turns into the switching.

The spin dynamics in the (1,1) bilayer differs significantly from the one in other bilayers. At first glance, it may seem that here we are dealing with a different mechanism of the switching. However, this is not the case. To explain the origin of this difference, we note that in the (1,1) bilayer the exchange scattering is less effective than in the ferrimagnetic alloys. For this reason the spin transfer between the RE and the TM sublattices slows down and can cause the switching only when the spin polarizations P_{RE} and P_{TM} are small. This explains why the switching in the (1,1) bilayer occurs at $T = 400$ K [Fig. 6(b)]. Along with the high temperature, the spin relaxation is necessary for the switching. At high-temperatures ($> T_A$) the equilibrium spin polarizations obey the relation $|P_{\text{RE}}^{\text{eq}}| < |P_{\text{TM}}^{\text{eq}}|$ and the switching without spin relaxation is impossible, see Fig. 3(b). Over time, the ratio between $P_{\text{RE}}(t)$ and $P_{\text{TM}}(t)$ can become reversed if the spin relaxation rate of TM ions is greater than that of RE ions. (For simplicity, we neglect at this point the spin polarization of the itinerant electrons.) This is exactly what happens in our case. In our model the relaxation of the localized spins occurs through the s - d interaction with the itinerant spins (the Korringa relaxation [21]). The spin relaxation rates of RE and TM ions scale as $\tau_{\text{RE}}^{-1} \propto \alpha_{\text{RE}}^2$ and $\tau_{\text{TM}}^{-1} \propto \alpha_{\text{TM}}^2$, respectively. Since we set $\alpha_{\text{RE}}/\alpha_{\text{TM}} = 0.1$ then $\tau_{\text{RE}}/\tau_{\text{TM}} \gg 1$. This means that the relaxation rate of TM spins is greater than that of RE spins. This confirms our assumption that at $T > T_A$ the initial relation $|P_{\text{RE}}^{\text{eq}}| < |P_{\text{TM}}^{\text{eq}}|$ goes with time into the opposite one $|P_{\text{RE}}(t)| > |P_{\text{TM}}(t)|$. Such a relation is necessary for the switching. Thus, we explain why the spin relaxation is necessary for the switching at temperatures above T_A . Note that the microscopic mechanism of the spin relaxation is not essential for the validity of the above conclusion.

The above analysis of the dynamics in the (1,1) bilayer allows us to draw a general conclusion concerning the temperature dependence of the switching. As we have shown (see also Ref. [18]) in the absence of spin relaxation, the switching is *possible* at temperatures exactly below T_A . Whether the switching occurs or not depends on other parameters of the system. Since the spin relaxation is always present in real systems the temperature range where the switching is possible shifts relative to T_A .

If the spin-relaxation rate of TM ions is greater than that of RE ions, then the temperature range where the switching is possible shifts to the higher temperatures. And vice versa, with the inverse ratio between the relaxation rates the temperature range shifts to the lower temperatures.

We also performed calculation of the dynamics for the ferromagnetic coupling between the layers ($J_{\text{TM-TM}} = 0.142$ and $J_{\text{RE-RE}} = J_{\text{TM-RE}} = 0.05$ eV). We did not find any switching; only demagnetization was observed (not shown).

Is interesting to compare our finding with the recent experimental study [22] of all-optical switching of ferrimagnet-ferromagnet heterostructures. In this heterostructure, a ferrimagnetic CoGd alloy film is exchange coupled

with Co/Pt multilayers (MLs). A Pt spacer fully blocks the nonlocal spin current, which is generated due to the ultrafast switching of the CoGd ferrimagnet. Nevertheless, the switching of Co/Pt MLs still occurs due to the indirect exchange coupling between the CoGd and Co/Pt.

The observed behavior is similar to the calculated switching dynamics in the (1,1) bilayer in that, in both cases, there is no spin current through the interface (spacer layer). At the same time, there is an essential difference.

The switching in the (1,1) bilayer is the collective, bidirectional process: no part of the bilayer can be switched independently of the other. As a consequence, the switching is possible only when the exchange coupling between the films is antiferromagnetic regardless of whether the interface is transparent for spins or not.

In contrast, in the ferrimagnet-ferromagnet heterostructures the CoGd film is switched by light independently of the ferromagnetic part of the heterostructure and then causes the Co/Pt MLs to switch. Thus, there is an asymmetry in the switching dynamics, and the switching is not a truly collective process. Therefore, the switching is possible for both ferromagnetic and antiferromagnetic types of exchange coupling.

IV. CONCLUSION

In conclusion, we calculated numerically the nonlocal laser-induced spin dynamics in the rare-earth/transition-metal bilayer. We focused on the role of spin transport in the magnetization switching. We considered the limiting cases of transparent and nontransparent interface between the layers and assumed that the spin transport is ballistic. The calculation is based on the Landau-Lifshitz-Bloch equation supplemented by the equations for the density of itinerant spins, electron, and phonon temperatures. To take into account the influence of spin transport on the spin dynamics, we used the approximate analytical expression for the spin splitting of electron chemical potential.

It was shown that the spin transport across interface strongly enhances the exchange scattering and facilitates the switching. We found that the switching is possible at the initial temperatures below a characteristic temperature T_f , which is not too far from the angular momentum compensation temperature. The temperature T_f can be either below or above T_A depending on the ratio between the spin-relaxation rates of RE and TM ions. Thus, in the case of transparent interface and ballistic spin transport the temperature dependence of the switching is similar to that in the ferrimagnetic alloys. This indicates that the exchange scattering plays a crucial role in the switching.

If the interface is nontransparent for the itinerant spins, the exchange scattering occurs only at the interface and becomes less effective. As a consequence, the switching occurs only in the (1,1) bilayer under the rather restrictive conditions.

Thus, our study shows that the spin transport is fundamental for achieving AOS in synthetic ferrimagnets. This finding is in agreement with the experiments [7–10].

- [1] C. Davies, J. Mentink, A. Kimel, T. Rasing, and A. Kirilyuk, Helicity-independent all-optical switching of magnetization in ferrimagnetic alloys, *J. Magn. Magn. Mater.* **563**, 169851 (2022).
- [2] P. Scheid, Q. Remy, S. Lebègue, G. Malinowski, and S. Mangin, Light induced ultrafast magnetization dynamics in metallic compounds, *J. Magn. Magn. Mater.* **560**, 169596 (2022).
- [3] A. El-Ghazaly, J. Gorchon, R. B. Wilson, A. Pattabi, and J. Bokor, Progress towards ultrafast spintronics applications, *J. Magn. Magn. Mater.* **502**, 166478 (2020).
- [4] M. L. M. Laliou, M. J. G. Peeters, S. R. R. Haenen, R. Lavrijsen, and B. Koopmans, Deterministic all-optical switching of synthetic ferrimagnets using single femtosecond laser pulses, *Phys. Rev. B* **96**, 220411(R) (2017).
- [5] M. Beens, M. L. M. Laliou, A. J. M. Deenen, R. A. Duine, and B. Koopmans, Comparing all-optical switching in synthetic-ferrimagnetic multilayers and alloys, *Phys. Rev. B* **100**, 220409(R) (2019).
- [6] L. Avilés-Félix, A. Olivier, G. Li, C. S. Davies, L. Álvaro-Gómez, M. Rubio-Roy, S. Auffret, A. Kirilyuk, A. V. Kimel, Th. Rasing *et al.*, Single-shot all-optical switching of magnetization in Tb/Co multilayer-based electrodes, *Sci. Rep.* **10**, 5211 (2020).
- [7] S. Iihama, Y. Xu, M. Deb, G. Malinowski, M. Hehn, J. Gorchon, E. E. Fullerton, and S. Mangin, Single-shot multi-level all-optical magnetization switching mediated by spin transport, *Adv. Mater.* **30**, 1804004 (2018).
- [8] Y. L. van Hees, P. van de Meughevel, B. Koopmans, and R. Lavrijsen, Deterministic all-optical magnetization writing facilitated by non-local transfer of spin angular momentum, *Nat. Commun.* **11**, 3835 (2020).
- [9] Q. Remy, J. Igarashi, S. Iihama, G. Malinowski, M. Hehn, J. Gorchon, J. Hohlfield, S. Fukami, H. Ohno, and S. Mangin, Energy efficient control of ultrafast spin current to induce single femtosecond pulse switching of a ferromagnet, *Adv. Sci.* **7**, 2001996 (2020).
- [10] S. Iihama, Q. Remy, J. Igarashi, G. Malinowski, M. Hehn, and S. Mangin, Spin-transport mediated single-shot all-optical magnetization switching of metallic films, *J. Phys. Soc. Jpn.* **90**, 081009 (2021).
- [11] M. Beens, R. A. Duine, and B. Koopmans, *s-d* model for local and nonlocal spin dynamics in laser-excited magnetic heterostructures, *Phys. Rev. B* **102**, 054442 (2020).
- [12] Ł. Cywiński and L. J. Sham, Ultrafast demagnetization in the *sp-d* model: A theoretical study, *Phys. Rev. B* **76**, 045205 (2007).
- [13] V. N. Gridnev, Landau-Lifshitz-Bloch equation for ferrimagnetic metals, *J. Magn. Magn. Mater.* **538**, 168241 (2021).
- [14] D. A. Garanin, Generalized equation of motion for a ferromagnet, *Physica A* **172**, 470 (1991).
- [15] P. Nieves, D. Serantes, U. Atxitia, and O. Chubykalo-Fesenko, Quantum Landau-Lifshitz-Bloch equation and its comparison with the classical case, *Phys. Rev. B* **90**, 104428 (2014).
- [16] P. Nieves, D. Serantes, and O. Chubykalo-Fesenko, Self-consistent description of spin-phonon dynamics in ferromagnets, *Phys. Rev. B* **94**, 014409 (2016).
- [17] V. N. Gridnev, Ferromagneticlike states and all-optical magnetization switching in ferrimagnets, *Phys. Rev. B* **98**, 014427 (2018).
- [18] V. N. Gridnev, Role of compensation points in all-optical magnetization switching, *Phys. Rev. B* **100**, 174405 (2019).
- [19] Since we neglect a magnetic field, our theory contains spins (or angular momenta) but not magnetic moments. As a consequence, the magnetization compensation temperature does not appear in any equations or conclusions of the theory.
- [20] $D = -1$ and -2 correspond to the complete demagnetization and switching, respectively.
- [21] J. Korringa, Nuclear magnetic relaxation and resonance line shift in metals, *Physica* **16**, 601 (1950).
- [22] J. Chatterjee, D. Polley, A. Pattabi, H. Jang, S. Salahuddin, and J. Bokor, RKKY exchange bias mediated ultrafast all-optical switching of a ferromagnet, *Adv. Funct. Mater.* **32**, 2107490 (2022).